Periodica Polytechnica
Civil Engineering

Parametric and Comparative Study of a Flexible Retaining Wall

62(2), pp. 295–307, 2018
https://doi.org/10.3311/PPci.10749

Aissa Chogueur[1*], Zadjaoui Abdeldjalil[1], Philippe Reiffsteck[2]

RESEARCH ARTICLE

Received 16 March 2017; Accepted 07 September 2017

Abstract

This paper presents design of a self-stabilizing retaining diaphragm wall, using conventional analytical calculation method based on subgrade reaction coefficient and by numerical method with finite elements method FEM can lead to various uncertainties. Hence, engineers have to calibrate a computational strategy to minimize these uncertainties due to numerical modeling. For both two methods, this paper presents various simulations with the structure installed into the supported ground without surcharge. For the first method, the analysis has investigate the influence of main factors such as the wall rigidity, the different stages of excavation, the Young's modulus, the cohesion and internal friction's angle of the soil. For the FEM method, two constitutive soil models are used such as Mohr-Coulomb MC and hardening soil model HSM. In case of the last model HSM, the variation of required and additional factors for the model was investigated as well as secant modulus stiffness $E^{ref}50$, unloading and reloading stiffness modulus E_{ur}, power factor m and Over-consolidated ratio OCR. The results from of the various simulations carried out are confronted with other experimental and numerical results [4]. Avery good coherence results are showed.

Keywords

centrifuge, diaphragm wall, finite elements, interface, numerical modeling, retaining wall, subgrade reaction

1 Department of Civil Engineering, RisAM Laboratory, Tlemcen University 22, Rue Abi Ayed Abdelkrim, Fg Pasteur BP 119. 13000, Algeria

2 IFSTTAR Paris, 14-20 Boulevard Newton, Cité Descartes Champs sur Marne, F-77447 Marne la Vallée Cedex 2, France.

* Correspondent author, email: most_chog@yahoo.fr

1 Introduction

The design of retaining walls in day-to-day practice is currently based on different calculation methods. If classical methods considering specific modes of failure, the elastic line and the equivalent beam are still employed for certain types of walls, it is mainly the subgrade reaction and the numerical methods which are most frequently adopted. The subgrade reaction method or spring method is rather well mastered and uncertainties mainly rely in the choice of the coefficient of subgrade reaction [1], [2]. The numerical methods have the advantage of taking into account more accurately the soil behavior, the soil-wall interface and also the ability to consider multiple hydraulic conditions and various options for modeling support conditions. However, the results obtained by these methods still require to be validated by engineer judgment or others experimental results (physical model in centrifuge for example) or measured in-situ. The main objectives of this study were to define the influence factors of the commonly used design methods and the resulting uncertainties encountered by the practitioners. This paper focuses on numerical modeling and analysis the behavior of a free standing diaphragm wall, made of reinforced concrete, embedded in sand, by the subgrade reaction method using the K-Rea software and by the numerical method based on finite elements with Plaxis 2D-v8.5 software. For both methods, different simulations have been performed with non-loaded supported soil. For the first method, we are interested in analyzing the influence of the main factors affecting soil movement and instability of the retaining wall. These factors mainly concern the wall rigidity, the construction sequence and mechanical parameters of the soil. One key step of this method is the difficulty in evaluating the coefficient of subgrade reaction Kh on a rational basis. Concerning the finite element method, the soil is homogeneous and dry; its behavior is described by linear elastic perfectly plastic model Mohr-Coulomb (MC) and nonlinear hardening soil model (HSM). The diaphragm wall is modeled by "beam" elements. The simulations were performed with different mesh sizes and reduction factors of the soil-wall interface. For both methods, the analyses are focuses on wall deformation,

bending moments and horizontal displacements. The results obtained, are confronted with well documented results [4].This paper summary the performance of this parallel formulation and results obtained from the simulation of this diaphragm wall. The computational strategy employed in this study offers practical approach for performing finite element simulations in day to day practice.

2 Historical overview

Physical modeling using centrifuge is a complementary way of study and research in addition to more theoretical approaches and tests on full-scale structures whose objectives are to study the behavior of geotechnical structures or dimensioning exceptional structures. During the year 1999, the British Geotechnical Society has ranked centrifuge modeling in the fifth place between the most important developments in geotechnical fields [5]. In this period, experimental works undertaken by Lyndon and Pearson, have studied the effect of the pressures on the structure during failure under rotational and translational kinematics [6] when Garnier et al., focused on the influence of wall's roughness on the structure behavior [7]. Bolton and Powerie have investigated the deformation and failure mechanisms of a rigid retaining structure during excavation at short and long term [8]. During the same year, Zhu and Yi used physical modeling tests to simulate real retaining structures [9]. Since the year 1994, the influence role of the structural elements on retaining wall behavior, was taken into account and we remind here especially the work of Powerie et al. that aimed at modeling the process of excavation installation and bracing of a diaphragm wall in clay [10]. In the same context, Schurmann and Jesberger have performed centrifuged tests to study the pressure profiles developed on a sheet piling driven into dry sand during excavation [11]. In the same period, a qualitative step forward was given to this technique and mainly relates to the first excavator device operating during flight for studying centrifuged excavations models developed by Kimura et al.; [12].This tool was used in other studies including those conducted by Takemura et al., [13]. During the year 1998, it became possible to study the three dimensional behavior of structure as done by Loh et al., to observe the behavior of two free standing retaining walls, stuck in a reconsolidated kaolin clay [14]. In practice, the tests conducted by Toyosawa et al., aimed at studying the possible failure mechanisms mobilizing the ruin of an anchored sheet piled model [15]. In 1999, a feasibility study has attempt, to establish a reduce thickness and an optimum instrumentation of wall to measure the satisfactory bending moments. Thanks to improvements given to centrifuges including the use of teleoperator during flight, Gaudin conducted experimental tests to study the behavior of a flexible and free standing retaining wall [4]. These works currently remain the reference for further researches on the behavior of this category of geotechnical structures. More recently, several researchers have pursued studying behavior of retaining walls but focused on seismic aspect using shaking table embedded in the centrifuge [16], [17], [18], [19], [20] and [21]. In order to point out of the evolution use of the centrifuge in the geotechnical fields, we have attempted to update the histogram showing the number of papers dealing with centrifuge experiments by categories of structure prepared by Corté and Garnier [22]. To do this, we gather information from wide articles recently published that focus particularly on physical modeling centrifuge. This histogram updated and given in figure1 is not exhaustive and has only an indicative value. It shows that tests on shallow foundations have kept their first position while those on retaining walls hold the same importance with much progress. Both, they represent the same greater percentage which is worth approximately 16 % from this range of articles. However, the deep foundations and slopes lose their rankings in first and second places. Down, they account for 13 % and 14 %. In the similar row, the buried pipe, tunnels and cavities represent separately the same percentage of 12%. With less progress, the trenches, reinforced soils, dams and embankments account for 4 % and 6 % of recent papers.

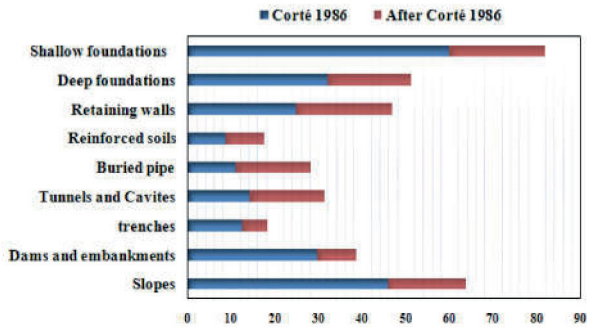

Fig. 1 Indicative distribution by type of works of publications dealing experiments in centrifuge (After Corté, 1986)

3 Model used for the benchmark

Due to the great step forward achieved by in IFSTTAR (Institut Français des Sciences et Technologies des Transport de l'Aménagement et des Réseaux) during experimental work on a reduced-scale model retaining wall, embedded into dry sand, to investigate its general behavior as well as interactions with a strip foundation [4], we have chosen these tests as reference for our numerical study.

3.1 Model description

The model wall reduced to 1/50th scale, was constituted of AU3G aluminium, 2 mm thick and 24 cm high, which thus represents a prototype wall 12 m in height (of which the first 10 m are embedded with a flexural rigidity EI equal to 6.54 MN.m^2 (corresponding approximately to an Arbed PU6 type profile). The model has been placed in a rectangular container 1200 × 800 × 360 mm in dimensions. 22 peers of strain gauge sensors

instrumented the central part of the wall. Measuring gauges gave directly the bending moment at the considered depth. Other instrumentation attached to the model allowed the determination, during the excavation, horizontal displacements of the wall, as well as settlement of supported earth. We note here that the centrifuge tests have been described in detail in [4].

4 Subgrade reaction coefficient method

In the first phase of this study, numerical simulations of this free-standing diaphragm wall were performed using the subgrade reaction method. These simulations were made using K-Rea software for modeling and analyzing the behavior. The calculation is based on the determination of the active/passive earth pressure coefficients. The literature suggests three main approaches to determine these coefficients; namely Coulomb, Rankine methods, Caquot-Absi and Kerisel tables. The subgrade reaction coefficient calculation can be made by three methods (Balay, Schmitt formulas and the Chadeisson abacuses). To find a better combination between these so-called calculating methods and subgrade coefficient determination methods, a preliminary comparative study was conducted. This confrontation with the computation results of numerical calculations, allows choosing of binomial methods, one for active and passive earth pressure coefficients calculation and another one for the subgrade reaction calculation. Once, the best combination between these methods is determined, we have proceeded with simulations to study the behavior of the wall which gave the results presented hereafter.

4.1 Review on subgrade modulus method

The simple and well-known subgrade reaction modulus method or "spring" method is still widely used and often preferred to more sophistically FEM analyses. This dependent pressures method uses one parameter Winkler analogue subsoil model. The contact soil is replaced by à system of independent elastic support of stiffness Kh. The wall is treated as an elastic beam of unit width and the value of the horizontal elastic soil reaction at examined point is directly proportional to horizontal wall displacement at the same point as is illustrated by the equation below:

$$P_z = K.y \leftrightarrow K = \frac{P_z}{y} \tag{1}$$

Where P_z the pressure stress at depth z and y is: is the horizontal displacement. It should be noted that Winkler's hypothesis is not based on any theoretical justification and that the reaction module cannot be considered as an intrinsic characteristic of the soil. Moreover, there is no rigorous method for determining their values. of course, the reaction modulus depends on the type of soil but it also depends on the configuration of the structure such as the value of the embedment height, the free wall height and the existence of anchor ties and the rigidity of the wall.

4.2 Analytic methods of subgrade reaction modulus K_h for walls

Various classical and empirical methods are known in specialized literature, they have been proposed for evaluating the coefficient K_h for retaining wall as Terzaghi, Rowe, Menard et al, Haliburton, Balay, and Chadeisson, Schmitt [2]. Most formulations established assume that K_h is directly proportional to the soil modulus E. In this paper, three of them shall be briefly discussed: Balay, Schmitt and chart of Chadeisson by separate approach to the problem.

4.2.1 Balay and Schmitt approaches

Both methods are based on the original method developed by Menard, Bourdon, Rousseau and Houy et al. [2] and [22], which derives K_h over the embedded length of a cantilever wall from pressuremeter modulus E_M:

$$K_h = \frac{E_M}{\left(\frac{\alpha.a}{2}\right) + 0.133(9a)^{\alpha}} \tag{2}$$

Where, a is a dimensional parameter as height in (m) defined by Menard at 2/3 of the embedded wall length, α is a rheological soil coefficient taken values 1/3 for non cohesive soil, 1/2 for silts and 2/3 for cohesive soils.

Balay adapted the Menard formulation for evaluating K_h over the entire wall length assuming a = H (free cantilever height) above the excavation level, while below the excavation ''a'' is related to the embedded length D and to the ratio D/H [3], [23].

On the other hand, Schmitt adapted the Menard formulation to take into account the flexural inertia of the wall EI by implementing the following formula:

$$K_h = \frac{2.10\left(\frac{E_M}{\alpha}\right)^{\frac{4}{3}}}{(EI)^{\frac{1}{3}}} \tag{3}$$

Early, Menard related empirically the pressuremeter modulus E_M to the elastic modulus of the soil by the ratio E_M/α. For normally consolidated soil α varies between 1/3 for sands and 2/3 for clays.

4.2.2 Chadeisson approach

The alternative approach proposed by Chadeisson as it is reported by Monnet consists in estimation of the subgrade reaction modulus value on the basis of the shear strength of the soil (cohesion c and friction angle φ), this proposal, takes the form of an abacus resulting from experimental results [2], [23]- fig.2. Subsequent to the experiences, justifications have been provided and published by Monnet, who proposes further developments to these propositions, while Londez et al illustrate the use of this Chadeisson abacus on a real structure [3].

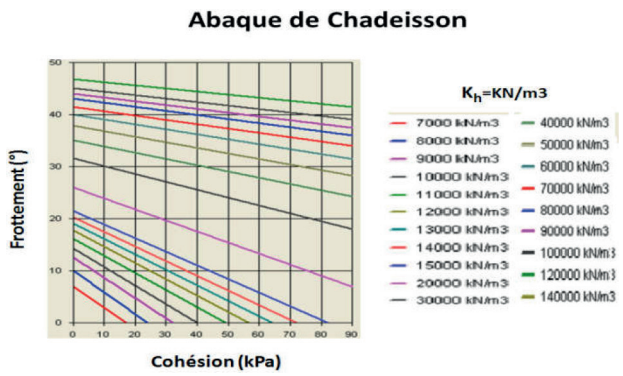

Fig. 2 Chadeisson curves- (K-Rea terrasol manual, 2006)

4.3 Mechanical Parameters of the Model

The material used for this method is Fontainebleau sand. This mono granular sand is commonly used in centrifuge or calibration chamber tests in France. It is fine and clean siliceous sand [4], its shear strength parameters are derived from drained and undrained triaxial (compression and extension) shear tests having the following characteristics:

γ (kN/m^3) = 16; c (kPa) = 2.6; φ (degree) = 39.4. For the diaphragm wall, an elastic law has been adopted, characterized by an elastic modulus E_{wall} =22.35 GPa, having an equivalent thickness of 15.2 cm and an embedded height of 10 m.

4.4 Design of the numerical model

Concerning the method of Balay, the soil is modeled by three layers having the same intrinsic parameters just to satisfy the usual recommendations for better choice of the value of the dimensional parameter ''a" However, for the other two approaches Schmitt and Chadeisson the soil is modeled by a Single layer. The excavation has six phases that each phase has a depth of 1m. For all three methods, the retaining wall is modeled by the same mechanical properties.

4.5 Results and interpretations

The results obtained from the different simulations as shown in the table 1 and figures 3, 4 and 5 below, suggest the following main conclusion:

It appears that the combination of the two separate methods of Rankine and Kerisel tables with Chadeisson abacuses, gave results very close to those obtained in centrifuge experiments for the test labeled A0-1[4]. The maximum bending moment estimated at 121kN.m/ml is also coherent with the experimental result with a slight difference for the maximum horizontal displacement estimated of 37 and 37.10 cm close to the 37.85 cm value obtained during experiments. Also, the Balay formula with Rankine method gives maximum bending moment estimated of 121kN.m/ml and in the same way maximum horizontal displacement was estimated of a 37.9 cm very close to 37.85 cm. The Schmitt formula strongly underestimated the results for the three methods, due to higher reaction coefficient. However the others methods give a close subgrade reaction K_h.

Hence, this coefficient from Schmitt formula is greater than those from Chadeisson and Balay methods. That is to say for example: 400821 < 52238 < 58411 for c = 2.6 kPa

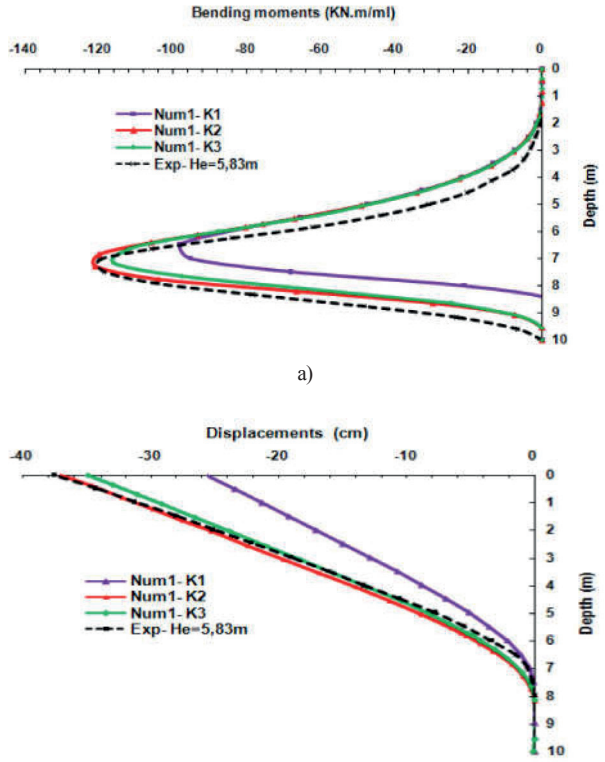

Fig. 3 Bending moments (a) and horizontal displacements(b) profiles obtained with K_h derived by the 3 studied methods (K1 Balay, K2 Schmitt and K3 Chadeisson) with Kerisel and Absi's tables

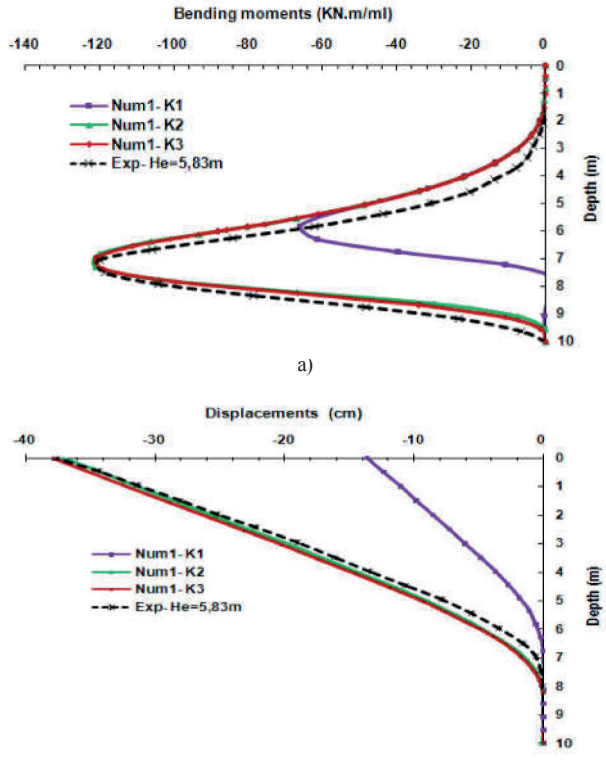

Fig. 4 Bending moments (a) and horizontal displacements (b) profiles obtained with K_h derived by the 3 studied methods (K1 Balay, K2 Schmitt and K3 Chadeisson) with Rankine's method

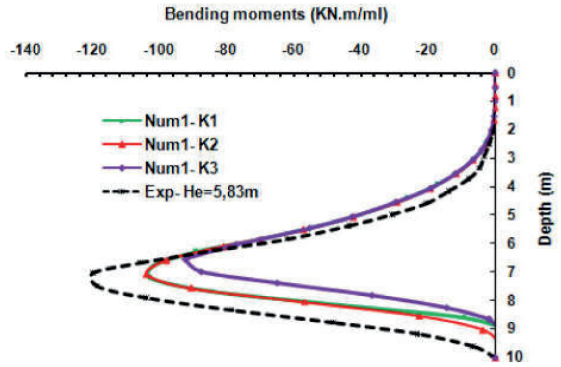

a)

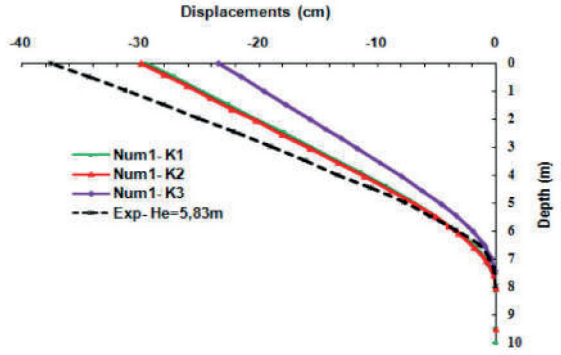

b)

Fig. 5 Bending moments (a) and horizontal displacements(b) profiles obtained with K_h derived by the three studied methods (Balay, Schmitt and Chadeisson) with Coulomb's method

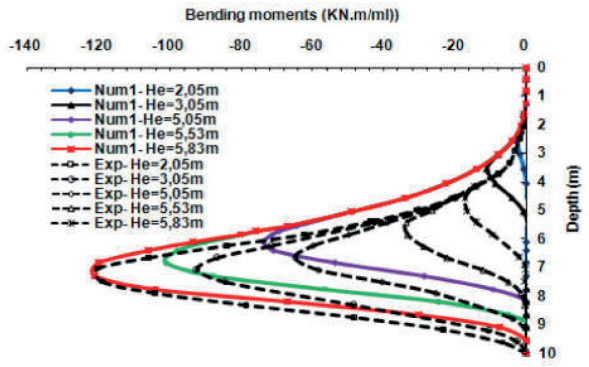

a)

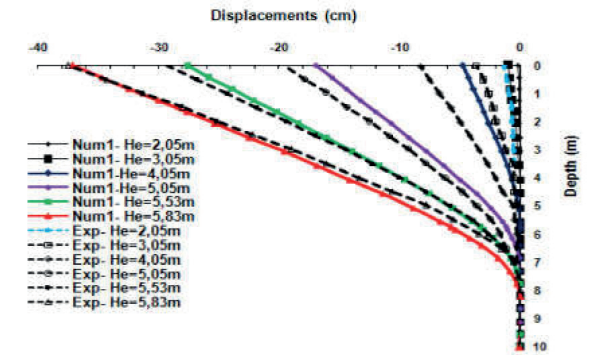

b)

Fig. 6 Bending moments (a) and horizontal displacements (b) profiles obtained with K_h derived by Chadeisson curves with Rankine's method

4.6 Validation on experimental results

For the second stage of the computations, the first combination using the Chadeisson's abacuses and the three methods is chosen in order to validate the experimental results. Various simulations are designed and performed to verify the convergence of calculations during the stages excavation to reach experimental heights 5.73 and 5.83 m corresponding to the experimental tests respectively noted A0-1 and A0-2 [4]. We present here only the results obtained by combining of the Rankine method with the Chadeisson's abacuses as it is illustrated according to Figure 6 below:

4.6.1 Interpretation and comments

The main conclusion drawn from these computations are that:

(a) As, the two heights of excavation (5.73 and 5.83 m) obtained during experiments are correctly verified, the diaphragm wall behavior is also correctly transcribed and it is generally consistent with experimental observations;

(b) The values of maximum bending moments are conform with experimental results and form part of the ranges of experimental values but they are underestimated at the beginning of excavation and especially for the first four stages;

(c) Maximum displacements corresponding to excavation heights 5.73 and 5.95 m, having respectively values of 27.20 and 33.6 cm, are underestimated of less than 20 and 32.80 % of the experimental results (34 and 50 cm) to estimate accurate lateral displacements.

Table 1 Results obtained by combining methods

	Exp	Balay formula			Schmitt formula			Abacuses Chadeisson		
		Coulomb	Rankine	Kerisel & Absi Tables	Coulomb	Rankine	Kerisel & Absi Tables	Coulomb	Rankine	Kerisel & Absi Tables
Height limit of excavation (m)	6.39	6.55	6.55	6.64	5.83	4.9	5.49	5.83	6.39	6.39
Maximum bending moments (kN.m/ml)	-120.9	-92.5	**-121**	**-116**	-103	-66.1	-98.2	-104	**-121**	**-121**
Maximum Horizontal displacements (cm)	-37.85	-23.4	**-37.9**	**-34.9**	-29.5	-13.6	-25.6	-29.9	**-37.1**	**-37**

5 Numerical modeling of the freestanding diaphragm wall using finite element method

5.1 Analysis with Mohr- Coulomb model

The numerical modelling of the retaining wall was performed using the Plaxis 2D.V8.5 software. The behaviour of soil is described by a linear elastic perfectly plastic model Mohr-Coulomb (MC) which involves five input parameters .i.e. E and v for soil elasticity, c and φ for plasticity and ψ as an angle of dilatance. This model is recommended to use for a first analysis of the problem considered [25].The diaphragm wall was modelled by "beam" element and not massive element as it has been used by Gaudin. There is place to note that the numerical model dimensions replicate those of the prototype structure and not the reduced-scale centrifuge model submitted to 50g acceleration. The geometrical dimensions chosen for this model are those advised for modelling in plane strain of an unsupported excavation with the maximum sizes [26], [27].These dimensions remain smaller than those established by Mestat who recommended a distance behind the wall of greater than six times the excavated height and advised a depth underneath the wall equal to four times the excavated height [28].The horizontal displacement for the vertical boundaries of the numerical model is zero (u = 0), as well as the vertical displacement along the lower boundary (v = 0). Four different kinds of meshes from coarse to dense were used to insure the reproducibility and minimize the divergence of the results. The reduction factor of interaction soil-wall (R_{inter}) has been chosen equal to 0.88 and 1.

5.2 Properties of soil

The soil consists of a single homogeneous layer of Fontainebleau dry sand. The analyses assume fully drained conditions throughout the profile and model the sand behavior using linearly elastic, perfectly plastic model with Mohr- Coulomb criteria. Two different values of cohesion c have been used and one value of internal friction's angle of soil φ .The parameters of E_{soil}, c, ψ and R_{inter} are variables according to the simulated case as indicated in the table 2.

Table 2 Properties of the soil layers and interfaces

E_{soil} (MPa)	v	c (kPa)	φ (°)	ψ (°)	R_{inter}
10	0.275	0–2.6	39.4	16.7	0.88–1.0

5.3 Properties of the diaphragm wall

The diaphragm wall is modeled by elastic beam elements. The properties of reinforced concrete are:

D(m) = 0.152; E_{wall} (MPa) = 22350; v = 0.3; H(m) = 10.

5.4 Simulation of construction and computed results

The soil structure interaction was analyzed in phases (staged construction) with plastic loading steps analysis using drained conditions. After the calculation of initial stresses and pore water pressures was completed, the excavation was simulated as shown in Fig.7 and like is detailed below:

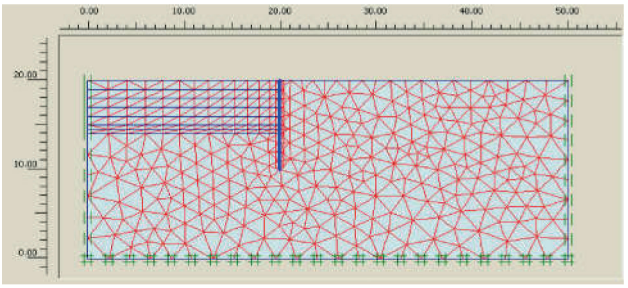

Fig. 7 Geometries and mesh used for the numerical model

Phase 1: There is no excavation, the wall is active; Phase 2: Excavation in 1m deep; Phase 3: Excavation in 2 m deep; Phase 4: Excavation in 3 m deep; Phase 5: Excavation in 4 m deep; Phase 6: Excavation in 5 m deep; Phase 7: Excavation in 5,83 m deep.

Table 3 Compared results of numerical simulations

	R_{inter}	Mesh type	Maximum bending moment (kN.m/ml)	Calculated result/ experimental Result (%)	Maximum horizontal displacements (cm)	Calculated result/ experimental Result (%)
E_{soil}= 10 MPa c = 0 kPa	1	Coarse	112.8	94%	34.11	90%
		Medium	115.54	96%	33.73	89%
		Fine	117.9	98%	33.95	89%
		Dense	120.8	101%	35.81	94%
	0.88	Coarse	119.22	99%	38.7	102%
		Medium	121.22	101%	37.8	99%
		Fine	117.8	98%	33.95	89%
		Dense	124.44	104%	38.92	102%
E_{soil}= 10 MPa c = 2.6 kPa	1	Coarse	58.54	49%	11.02	29%
		Medium	60.34	50%	11.34	30%
	0.88	Medium	62.88	52%	15.28	40%
		Fine	65.5	55%	15.28	40%

We present here after only the results obtained by the simulations performed to verify the convergence of calculations during the phase's excavation until reaching the experiment height of 5.83 m. We specify that the inserted abbreviations at the end of the paper are used.

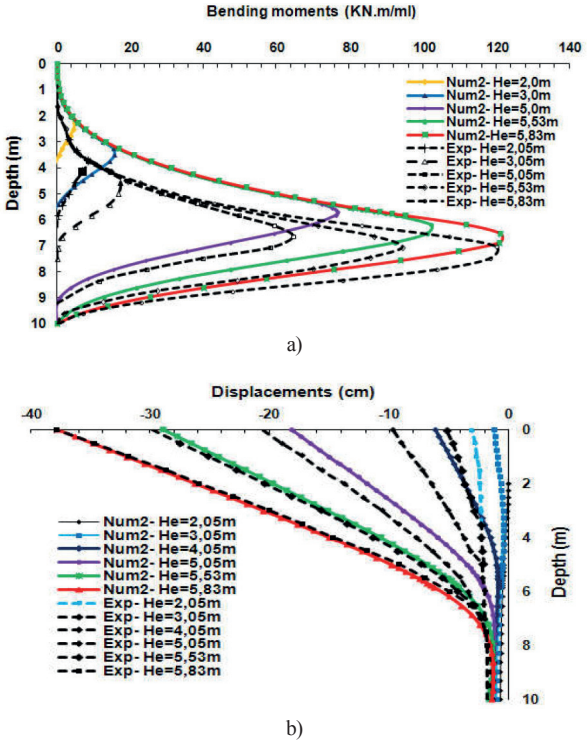

Fig. 8 Bending moments (a) and horizontal displacements (b) profiles versus heights of excavation with E_{soil} = 10 MPa, c = 0 kPa and R_{inter} = 0.88

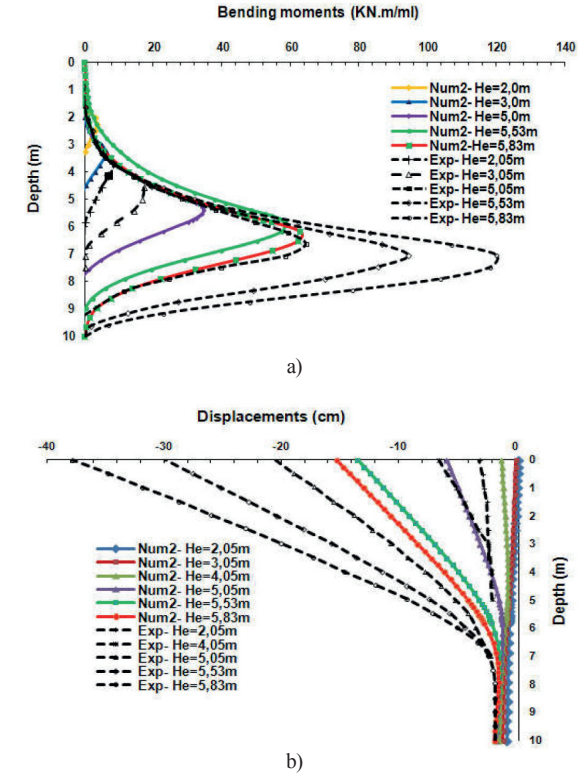

Fig. 9 Bending moments (a) and horizontal displacements (b) profiles heights of excavation with E_{soil} = 10 MPa, c = 2.6 kPa and R_{inter} = 0.88

5.5 Interpretation and comments

The main results drawn from these computations are:

(a) The experimental height of excavation (5.83 m) is correctly estimated.

(b) The diaphragm wall behavior is correctly transcribed and it is over all in conformity with the one observed in the experimental tests (profiles of the horizontal displacement and bending moments).

(c) The profiles of displacements at the head illustrate clearly the level of embedment length which is located between 6 m and 10 m. Indeed, the deformation affects only the party above the bottom of the excavation.

A For a zero soil's cohesion

For soft contact (R_{inter}), the values of maximum bending moments are underestimated in the case of "Coarse, medium and fine" meshes. In the three cases, the differences do not exceed 6 %. As against, in the case of a dense mesh, a light over-estimation has been recorded (about 1 %) and more is dense the mesh more the computed values are overestimated. Indeed, for a sliding contact (R_{inter} < 1), it appears that the values obtained according to the mesh type have a little influence on the results but the interaction coefficient of reduction directly affects the retaining wall behavior. In the other hand, the values of maximum horizontal displacements are ranged in an interval from -11 % to 7 % compared to the experimental result. However, for soft contact (R_{inter} =1), the values are underestimated from -11 % to -6 %.

B For a nonzero soil's cohesion

The maximum values of bending moments range in an interval of (-51 to -45 %) when those for maximum horizontal displacements range also in an interval from (-71 to -60 %) compared to experimental result. In the same way, more the mesh is denser more the underestimation of the results decreases. The elastic modulus and the interaction coefficient of reduction have little influence on the computation results.

In conclusion, for a soil cohesion "c = 0 kPa" using a sliding contact (R_{inter} <1), the computation results are satisfactory and at least two results are consistent with experimental results. However, for the cohesion of the soil "c = 2.6 kPa", the results are strongly underestimated whatever the type of contact.

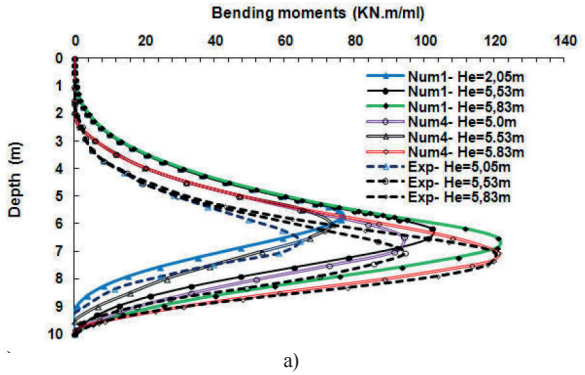

a)

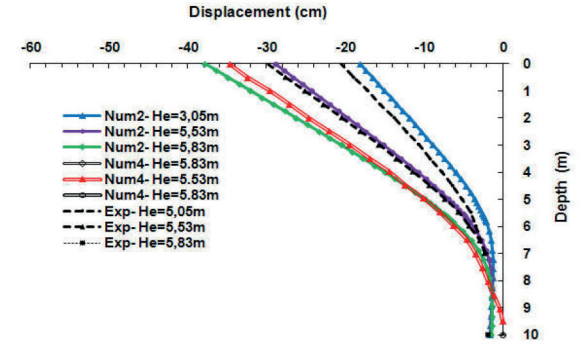

b)

Fig. 10 Comparison between profiles of bending moments (a) and displacements (b) for different heights of excavation

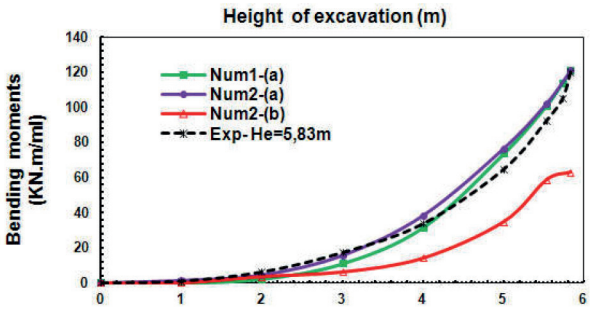

a)

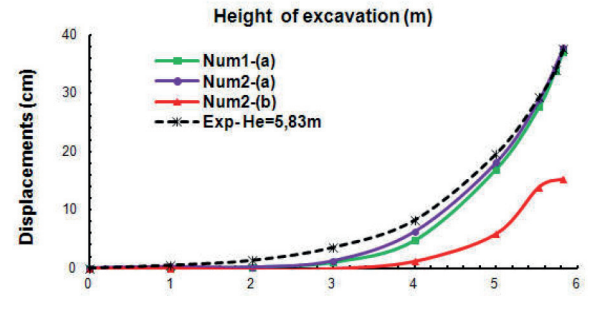

b)

Fig. 11 Comparison between profiles of bending moments (a) and displacements (b) for H_e = 5.83 m

6 Analysis with Hardening soil model HSM

6.1 Brief presentation of the hardening soil model

The hardening soil model (HSM) implanted in Plaxis software is derived from the hyperbolic model of Duncan and Chang [30] with some improvement on the hyperbolic formulations in elasto-plastic framework [25]. Initially, this model isotropic is an extension of the Mohr-Coulomb model [32]. More accurately, the total strains are calculated using soil stiffness by using three different stiffness, i.e. triaxial loading secant stiffness E_{50}^{ref}, triaxial unloading/reloading stiffness E_{ur}^{ref} and oedometer loading tangent stiffness E_{oed}^{ref} at the reference pressure P^{ref} that usually taken as 100kPa. For sand soil (c = 0 kPa), the three stiffness modulus for different confining effective stresses can be defined by the equations bellows:

$$E_{50} = E_{50}^{ref}\left(\sigma_3' / P^{ref}\right)^m \tag{4}$$

$$E_{oed} = E_{oed}^{ref}\left(\sigma_3' / P^{ref}\right)^m \tag{5}$$

$$E_{ur} = E_{ur}^{ref}\left(\sigma_3' / P^{ref}\right)^m \tag{6}$$

Where E_{oed}^{ref} and E_{ur}^{ref} are respectively assumed to be equal to E_{50}^{ref} and $3E_{50}^{ref}$ by default [25]. Where σ_1' and σ_3' are the major and minor principal effective stresses. More the three stiffness modulus, other parameters are required as power for stress m defined by user, lateral stress coefficient deduced from Jacky's formula (K_0^{nc}=1-sin φ), friction angle φ, dilatance angle ψ from triaxial tests investigations, unloading / reloading Poisson's ratio v_{ur} and failure ratio R_f taken values respectively of 0,2 and 0,9 by default [25]. The formulations and verification of the model are explained in detail by Schanz et al. [31] and Brinkgreve [25]. It should be pointed out that the HSM is suitable for all types of soil.

6.2 Calculation process

The same numerical model and calculation process as in the case of the MC model were also considered in the analysis of the behavior of the retaining wall with hardening soil model HSM. Exceptionally, the required input parameters of the model are again implemented. Since the parameters E_{50}^{ref}, E_{ur}^{ref}, m and OCR are important input data of the HSM model; four cases of parametric studies have been developed to evaluate the sensitivity of these parameters on prediction of wall movements.

As first choice, the sensitivity of E_{ur}^{ref} is analysed with simulations taken in account the initial fixed value of the secant modulus E_{50}^{ref} = 18 MPa while the ratio $\frac{E_{ur}^{ref}}{E_{50}^{ref}}$ had values of 2.5, 3, 4 and 5. Considering $E_{oed}^{ref} = E_{50}^{ref}$ the four correlations obtained lead to the corresponding calculated data input for unloading and reloading modulus summaries in table 5 below.

For the second choice, the sensitivity of E_{50}^{ref} is analyzed with simulations taken in account the variation of the initial value of the secant modulus E_{50}^{ref} = 18 MPa which was multiplied by a variable factor of 0.50,1,1.50 and 2 giving respectively values of 9 MPa, 18 MPa, 27 MPa and 36 MPa. Also considering $E_{oed}^{ref} = E_{50}^{ref}$, the correlation recommended ($E_{ur}^{ref} = 3E_{50}^{ref}$) leads to the calculated input data for unloading and reloading modulus summaries in table 6 below.

Concerning the third and the fourth choices relating to the sensitivity of the two parameters "m" and "OCR", the initial value of E_{50}^{ref} remains unchanged. However, the parameter "m" had arbitrary values of 0.3, 0.5, 0.7 and that of OCR held values of 1, 1.5, 2.5 and 5 [4]. Therefore, the corresponding input data are also shown in the tables 4, 5, 6, 7 and 8. It is reported that the numerical data identified by an asterisk (*) are retrieved from paper published by Sheil Brian et al. In coming, only the results relate the last phase are presented.

Table 4 Fixed soil characteristic for Fontainebleau sand

γ(kN/m³)	γ_{sat}(kN/m³)	c (kPa)	φ (°)	Ψ(°)
16	19.85	0	39.4	16.7

Table 5 Input Data for E_{ur}^{ref} – – Choice n°01

E_{50}^{ref} (MPa)	E_{oed}^{ref} (MPa)	E_{ur}^{ref} (MPa)	m	OCR	v_{ur}
18*	18*	45* 54 72 90	0.5	1	0.2

Table 6 Input Data for – Choice n°02

Factor	0.5	1	1.5	2
E_{50}^{ref} (MPa)	9	9	27	36
$E_{ur}^{ref} = 2\,E_{50}^{ref}$ (MPa)	18*	18*	54	72
$E_{ur}^{ref} = 3\,E_{50}^{ref}$ (MPa)	27	27	81	108
$E_{ur}^{ref} = 4\,E_{50}^{ref}$ (MPa)	36	36	108	144
m		0.5		
OCR		1		
v_{ur}		0.2		

Table 7 Input Data for power "m" – Choice n°03

E_{50}^{ref} (MPa)	E_{oed}^{ref} (MPa)	E_{ur}^{ref} (MPa)	m	OCR	v_{ur}
18*	18*	45*	0.3 0.5 0.7	1	0,2

Table 8 Input Data for OCR – Choice n°04

E_{50}^{ref} (MPa)	E_{oed}^{ref} (MPa)	E_{ur}^{ref} (MPa)	m	OCR	v_{ur}
18*	18*	45*	1, 1.25, 2.5, 5	0.5	0.2

6.3 Interpretation and comments

The results obtained from the different simulations as shown in the figures from 12 to 18 below, suggest the following main conclusion:

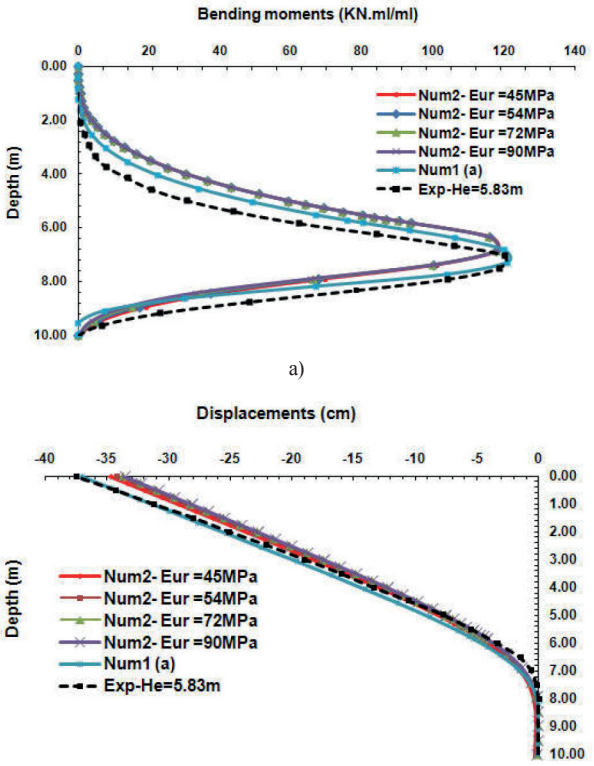

Fig. 12 Analysis of efficiency of unloading and reloading modulus E_{ur} on bending moments (a) and displacements (b) - HSM

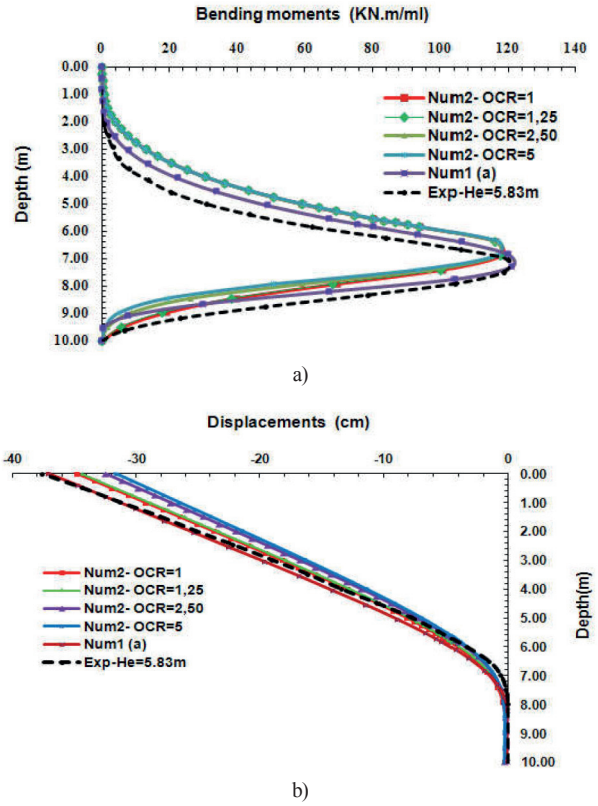

Fig. 13 Analysis of the influence of the overconsolidation ratio OCR on bending moments (a) and displacements (b) - HSM- E_{ur} = 45MPa

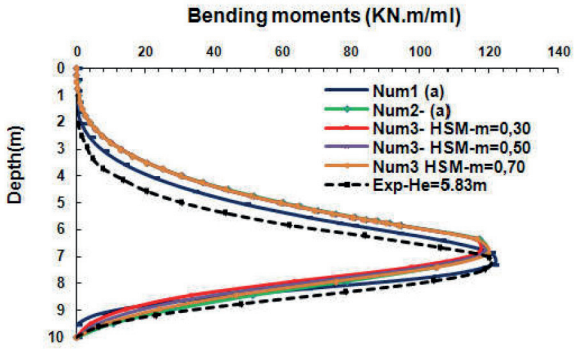

a)

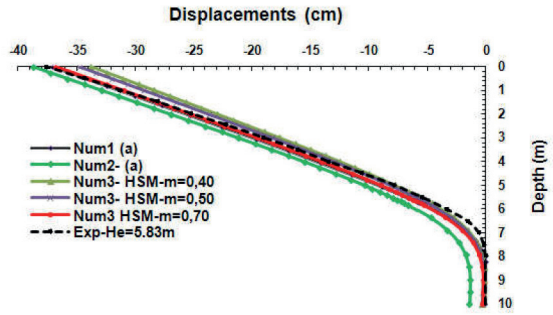

b)

Fig. 14 Analysis of the influence of the power factor "m" bending moments (a) and displacements (b) - HSM- E_{ur} = 45MPa

6.3.1 Analysis of the influence of E_{50}^{ref} parameter

The observations on figures 17 and 18 show clearly the important effect of the secant modulus E_{50}^{ref} on the movements of the retaining wall. The increasing variation of this parameter produces decreasing results. Hence, the bending moments decrease slightly in a margin between +0.2 % and -3 % compared with those experimental when the lateral displacements decrease in a margin between +1 % and -17 %. The effect of the ratio $\frac{E_{ur}^{ref}}{E_{50}^{ref}}$ with $E_{oed}^{ref} = E_{50}^{ref}$ is really observed. The quantity $\frac{E_{ur}^{ref}}{E_{50}^{ref}} = 3$ gave results in good coherence with those experimental, contrary to the quantity $\frac{E_{ur}^{ref}}{E_{50}^{ref}} = 2$ which gave underestimated results. On the other hand the quantity $\frac{E_{ur}^{ref}}{E_{50}^{ref}} = 4$, slightly overestimate the calculated results. Then, it is distinguished that the parameter E_{50}^{ref} is purely a shear parameter of the HSM model and that the quantity $\frac{E_{ur}^{ref}}{E_{50}^{ref}} = 3$ recommended by Brinkgreve [25] remains effective to describe the behavior of the wall in interaction with the supported soil.

6.3.2 Analysis of the influence of the E_{ur} parameter

Compared to the experimental results, the computed results relating to bending moments and lateral displacements decrease with the excessive increase of the values of the parameter E_{ur} from 45 to 90 MPa – see figure 12. The bending moments decrease slightly in a margin between -2 % and -1 % when the horizontal displacements decrease roughly within a margin between -10 % and -7 % So, the minimum value E_{ur} = 45 MPa produced results in good coherence with the those experimental, this one makes 4.50 times of the initial Young's modulus of the soil (E_{sol} = 10 MPa) considered in the calculations with the MC model. From other simulations carried out, it appears that more the value of E_{ur} becomes lower and approximates the value of the initial module E_{sol}, more the computed results increase. In addition the maximal surface of settlements is distinguished affected by this same low value -see figure 15. It must be retained that the variation of the parameter E_{ur} controlled by the shear parameters c and φ, directly and absolutely affects the behavior of the retaining wall.

6.3.3 Analysis of the influence of the OCR ratio parameter

It is well apparent from the observations on figure 13 that the influence of the OCR parameter is important and remarkable. The computed results decrease with margins greater than those observed for the other two parameters E_{50}^{ref} and E_{ur}. Hence, the bending moments and lateral displacements results decrease in margins respectively from -2 % to -1 % and -15 % to -7 %. The increasing transition from the normally consolidated state to the overconsolidation stages (variation of the OCR ratio from 1 to 5), explains the effect of the plasticity state of the soil around the wall. Hence, the maximum settlements area induced by the wall displacement at the top is distinguished by effect of the highest value of the OCR ratio- see figure 16.

6.3.4 Analysis of the influence of the power parameter "m"

Unlike the other three E_{50}^{ref} , E_{ur} and the OCR ratio parameters, the parameter "m" distinguishes itself directly influencing the computed results. Indeed, the bending moments increase in a margin between -2 % and 0.2 % while the lateral displacements also increase in a margin between -11 % and -2 %. i.e. the calculated results increase proportionally with the increase of the value of "m" from 0, 3-0, 5 and 0.7. Due to close calculated values, Profiles are slightly superposed especially for the bending moments but for the lateral displacements are quite dispersed- see figure 14.

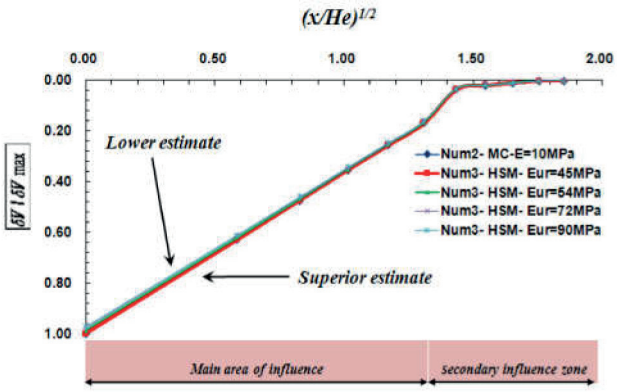

Fig. 15 Analysis of the influence of stiffness unloading and reloading modulus E_{ur} on surface settlement with OCR=1

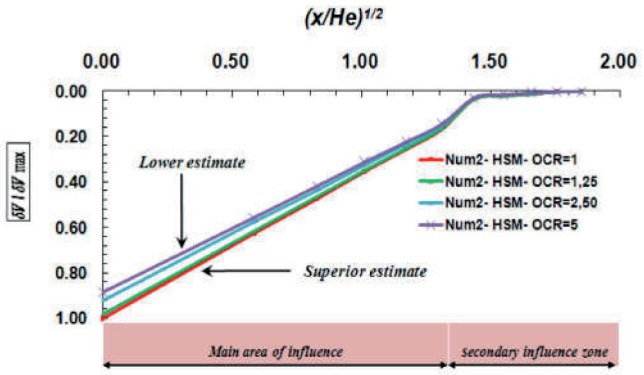

Fig. 16 Analysis of the influence of the over consolidation ratio OCR on surface settlements with E_{ur} = 45 MPa

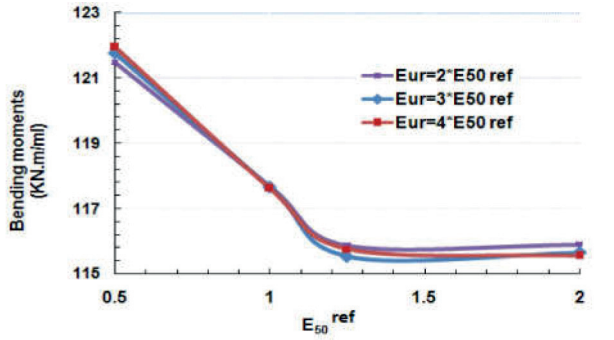

Fig. 17 Effects of the secant modulus E_{50}^{ref} on bending moments

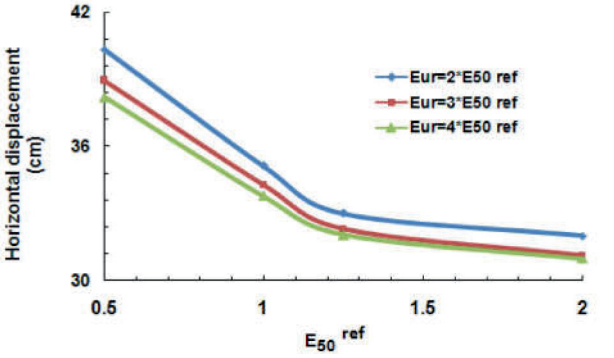

Fig. 18 Analysis of the influence of the secant modulus E_{50}^{ref} on horizontal displacements

7 Conclusions

It emerges from this parametric and comparative study the following conclusions:

(a) For each excavation stage, a very good consistency was found between the calculated values and the values recorded in experiments; this observation is valid for the retaining wall behavior, lateral displacements and bending moments. However, it was noted a slight overestimation for maximum excavation heights compared to the experimental results.

(b) About the methods used for estimation of the experimental excavation height, the results obtained are in good agreement with the experimental results. However, it is observed an underestimation of the results of bending moments especially in the first four stages and overestimation beyond the fourth stage. Similarly an underestimation of the horizontal displacements is obtained for all stages except the last one.

(c) The finite element method using MC and HS models with a zero cohesion, seems more powerful and it gave closer results to those obtained experimentally especially for the first four stages. At the time, the subgrade reaction using Chadeisson approach with Rankine's theory satisfied similar closer results but in paradox like finite element method (MEF), the results are strongly underestimated for a zero soil's cohesion. Unfortunately there is no explanation of this contradiction between the two methods.

(d) The results obtained are in good consistency with those made by YAP et al [28]. Indeed, the comparative results show that in terms of distribution and magnitude of active earth pressure, Rankine's theory possesses the highest match to the Plaxis analysis and also it has the highest compatibility to finite element analysis among all theories.

(e) The lateral displacements obtained by using MC model (linear elastic) are not realistic because the stiffness is taken constant while those obtained by non linear hardening soil model (HSM) are more realistic. Hence, the HSM can present more accurately results when the correct values of required parameters are carefully chosen as well as the secant modulus E_{50}^{ref} unloading and reloading modulus E_{ur}, over consolidation ratio and power factor "m"…

Abbreviations

A0-1	First test completed by Gaudin
A0-2	Repetition of A0-1 test.
c	Soil's cohesion
d	Equivalent thickness of wall
E_{soil}	Young's modulus of soil
E_{wall}	Young's modulus of wall
E_{xp}	Experimental results.
FEM	Finite element method.
H_e	Height of excavation.
K_1	Numerical computations with Num1 using Rankine method and K_h according to Schmitt formula at H_e limited = 4.90m
K_2	Numerical computations with Num1 using Rankine method and K_h according to Chadeisson chart at H_e = 5.83m
K_3	Numerical computations with Num1 using Rankine method and K_h according to Balay formula at H_e = 5.83m
K_h	Subgrade reaction coefficient
Num1	Numerical computations with Subgrade reaction method using K-Rea software
Num1 (a)	Numerical result with Num1 at H_e = 5.83m
Num2	Numerical computations with FEM using MC model using Plaxis 2D

Num2 (a)	Numerical result with Num2 at H_e=5.83m for E = 10MPa and c=0 kPa
Num2 (b)	Numerical result with Num2 at H_e=5.83m for E = 10MPa and c=2.60 kPa
Num3	Numerical computations with FEM using HSM model using Plaxis 2D
Num4	Numerical computations with FEM using LCPC Cesar software
R_{inter}	Strength reduction factor interaction
ν	Poisson's ration
γ	Soil unit weight
φ	Friction angle
Ψ	Dilatancy angle

References

[1] Szepesházi, A., Mahler, A., Móczár, B. "Three Dimensional Finite Element Analysis of Deep Excavations Concave Corners". *Periodica Polytechnica Civil Engineering,* 60(3), pp. 371–378. 2016. https://doi.org/10.3311/PPci.8608

[2] Delattre, L. "Un siècle de méthodes de calcul d'écrans de soutènement partie I.L'approche par le calcul, les méthodes classiques et la méthode au coefficient de réaction" (A century of calculation methods for retaining shields part I. The calculation approach, classical methods and the reaction coefficient method) *Bulletin des Labortoires des Ponts et Chaussées,* 234, pp. 35–55. 2001. http://www.ifsttar.fr/collections/BLPCpdfs/blpc_234_35-56.pdf

[3] Monnet, A. "Module de réaction, coefficient de décompression, au sujet des paramètres utilisés dans la méthode de calcul élastoplastique des soutènements" (Reaction module, decompression coefficient, concerning the parameters used in the elastoplastic calculation method of the supports). *Revue Française de Géotechnique,* 65, pp. 67–72. 1994. http://www.geotech-fr.org/sites/default/files/rfg/article/66-6.pdf

[4] Gaudin, C. "Modélisation physique et numérique d'un écran de soutènement auto stable, application à l'étude de l'interaction écran-fondation" (Physical and numerical modeling of a self-supporting retaining screen, application to the study of screen-foundation interaction). Thèse de doctorat, École Centrale de Nantes, France. 2002.

[5] Charles, W, W, NG. "The state-of-the-art centrifuge modelling of geotechnical problems at Hkust." *Journal of Zhejiang University-SCIENCE A (Applied Physics & Engineering),*15(1), pp. 1–21. 2014. https://doi.org/10.1631/jzus.A1300217

[6] Lyndon, A., Pearson, R. A. "Pressure Distribution on Rigid Retaining Wall in Cohesionless Material." In: *Proceedings of International Symposium of Centrifuge Modelling to Geotechnical Design*. (Balkema, A. (Ed.)). pp. 271–280. 1985.

[7] Garnier, J., Derkx, F., Cottineau, L. M., Rauh, G. "Etudes géotechniques sur modèles centrifugés: Evolution des matériels et des techniques expérimentales" (Geotechnical studies on centrifuged models: Evolution of materials and experimental techniques). *Bulletin des labortoires des ponts et chaussées,* 223, pp. 27–50. 1999. http://www.ifsttar.fr/collections/BLPCpdfs/blpc__223_27-50.pdf

[8] Bolton, M. D., Powerie, W. "Behaviour of diaphragm walls in clay prior collapse". *Géotechnique,* 38(2), pp. 167–189.1988. https://doi.org/10.1680/geot.1988.38.2.167

[9] Zhu, W., Yi, J. "Application of Centrifuge Modeling To Study a Failed Quay Wall." In: *Centrifuge 88.* (Corte J. F. (Ed.)). pp. 415–419. Balkema, Rotterdam. 1988.

[10] Powerie, W., Richards, D. J., Kantartzi, C. "Modelling Diaphragm Wall Installation and Excavation Processes". In: *Centrifuge 94: proceedings of the International Conference Centrifuge,* 1994, Singapore, 31. August – 2 September 1994. Balkema, pp. 655–661. 1994.

[11] Schurmann, A., Jesseberger, H. L. "Earth Pressure Distribution on Sheet Pile Walls" In: *Centrifuge 94: Proceedings of the International Conference (*Leung, Lee and Tan, T. S. (Eds.)). pp. 95–100. Defense Technical Information Center, 1994.

[12] Kimura, T., Takemura, J., Hiro-Oko, A., Okamura M., Park, J. "Excavation in soft clay using an in-flight excavator". *Centrifuge 94. (*Leung, Lee and Tan, T. S. (Eds.)). pp. 649–654. Defense Technical Information Center, 1994.

[13] Takemura, J., Kondoh, M, Esaki, T., Kouda, M., Kusakabe, O. "Centrifuge Model Tests on Double Propped Wall Excavation in Soft Clay". *Soils and foundations, 39*(3), pp. 75–87.1999. http://doi.org/10.3208/sandf.39.3_75

[14] Loh, C. K., Tan, T. S., Lee, F. H. "Three-Dimensional Excavation Tests". In: *Proceedings of the International Conference Centrifuge 98'*, Tokyo, Japan, pp. 649–654. 1998.

[15] Toyosawa, Y., Horrii, N., Tamate, S., Suemasa, N., Katada, T. "Failure mechanism of anchored retaining wall." In: *Proceedings of the International Conference Centrifuge 98'*, Tokyo, Rotterdam, Belkema, pp. 667-672. 1996. https://scholar.google.fr/scholar?hl=fr&q=Failure+Mechanism+of+Anchored+Retaining+Wall

[16] Matsuao, O., Nakamura, S. Saito, Y. "Centrifuge Test on Seismic Behaviour of Retaining Walls", Physical Modelling in Geotechnics. Phillips vd. eds. Rotterdam: Balkema. pp. 453-458. 2002

[17] Sitar, N., Al Atik, L. "Dynamic centrifuge study of seismically induced lateral earth pressures on retaining structures". In: *Geotechnical Earthquake Engineering and Soil Dynamics Congress, IV.* (Zeng, D., Manzari, M. T., Hiltunen, D.,R. (Eds)). pp. 1–11. Sacramento, California, United States, ASCE, 2008. https://doi.org/10.1061/40975 (318)149

[18] Morikawa, Y., Takahashi, H., Hayano, K., Okusa Y. "Centrifuge Model Tests on Dynamic Behavior of Quay Wall Backfilled with Granular Treated Soil". In: *Proceedings 8th International Conference on Urban EarthquakeEngineering,* pp. 279–284. 2011. https://doi.org/10.1061/9780784413272.344

[19] Greco, V. R. "Reexamination of Mononobe-Okabe theory of gravity retaining Walls using centrifuge model tests". *Soils and Foundations,* 47(5), pp. 999–1001. 2007. http://doi.org/10.3208/sandf.47.999

[20] Agusti, G. C., Sitar N. "Seismic earth pressures on retaining structure in cohesive soils". Report No. UCB GT 13-02. Civil and Environmental Engineering University of California-Berkeley. 2013. http://www.dot.ca.gov/hq/esc/earthquake_engineering/Research_Reports/vendor/uc_berkeley/Final_Report_65A0367_Cohesive.pdf

[21] Dashti, S., Hushmand, A., Ghayoomi, M., McCartney, J.S., Zhang, M., Hushmand, B., Mokarram, N., Bastani, A., Davis, C., Lee, Y, Hu J. "Centrifuge Modelling of Seismic Soil-Structure-Interaction and Lateral Earth Pressures for Large Near-Surface Underground Structures." In: *Proceedings of the 18th International Conference on Soil Mechanics and Foundation Engineering*, pp. 899–902. 2013. http://www.cfms-sites/all/lic/pages/download_pdf.php?file=899-902.pdf

[22] Corte, J. F., Garnier, J. "Une centrifugeuse pour la recherche en géotechnique" (Centrifuge for geotechnical research). *Bulletin des labortoires des ponts et chaussées,* 146, pp. 5–28. 1986.

[23] K-Réa v4. Manuel d'utilisation. Edition 2016. http://www.terrasol.fr/fr/logiciels/ logiciels-terrasol/k-rea-v4

[24] Fixot, J. "Analyse comparative de la norme NF P 94 282 sur les écrans de soutènement". Génie civil, 2013. https://dumas.ccsd.cnrs.fr/dumas-01143111/document

[25] Brinkgreve, R. B. J. "Manual of Plaxis 3D-2012." Delft University of Technology Plaxis BV, The Netherlands. 2012.

[26] Cheang, W. "Part 1: Geometry space, boundaries and meshing. Part 2: Initial stresses and Phi-c reduction". Advanced Computational Geotechnics, Plaxis Vietnam Seminar. 2008. https://fr.scribd.com/document/290822898/Lecture-3

[27] Cheang, W. "Modeling of excavation using Plaxis". Advanced Computational Geotechnics, Plaxis Vietnam Seminar. 2008. https://fr.scribd.com/document/290822898/Lecture-3

[28] Mestat, P. "Maillage d'éléments finis pour les ouvrages de géotechnique, conseils et recommandation" (Finite Element Mesh for Geotechnical Structures, Advice and Recommendation). *Bulletin des laboratoires des ponts et chaussées,* 212, pp. 39–64. 1997.

[29] Yap, S. P., Salman, F.A., Shirazi, S.M. "Comparative study of different theories on active earth pressure". *Journal of Central South University,* 19(10), pp. 2933–2939. 2012. https://doi.org/10.1007/s11771-012-1361-2

[30] Duncan, J. M., Chang, C. Y. °Nonlinear Analysis of Stress and Strain in Soils". *Journal of Soil Mechanics and Foundation Division,* 96(5), pp. 1629–1653. 1970.

[31] Schanz, T., Vermeer, P. A., Bonnier, P. G. "The hardening soil model: formulation and verification". In: Beyond 2000 in Computational Geotechnics, 10 years of plaxis. pp. 1–16. Balkema. 1999.

[32] Nordal, S. "Present of Plaxis". In: Beyond 2000 in Computational Geotechnics, 10 years of plaxis International. pp. 45–54. Balkema. 1999.

[33] Sheil, B. B., McCabe, B. A. "Biaxial loading of offshore monopiles: numerical modeling." *International Journal of Geomechanics,* 17(2), pp. 5–6. 2016. https://doi.org/10.1061/(ASCE)GM.1943-5622.0000709